IMPROVEMENT OF SPATIAL RESOLUTION WITH STAGGERED ARRAYS AS USED IN THE AIRBORNE OPTICAL SENSOR ADS40

R. Reulke[a], U. Tempelmann[b], D. Stallmann[c], M. Cramer[a], N. Haala[a]

[a] Institute for Photogrammetry (ifp), Stuttgart University, Germany - ralf.reulke@ifp.uni-stuttgart.de
[b] Leica Geosystems GIS & Mapping GmbH, Heerbrugg, Switzerland - udo.tempelmann@gis.leica-geosystems.com
[c] Stuttgart, Germany - dirk.stallmann@o2online.de

Commission I, WG I/4

KEY WORDS: photogrammetry, geometry, calibration, modeling, aerial sensor, digital, three-line, pushbroom

ABSTRACT:

Using pushbroom sensors onboard aircrafts or satellites requires, especially for photogrammetric applications, wide image swaths with a high geometric resolution. One approach to satisfy both demands is to use staggered line arrays, which are constructed from two identical CCD lines shifted against each other by half a pixel in line direction. Practical applications of such arrays in remote sensing include SPOT, and in the commercial environment the Airborne Digital Sensor, or ADS40, from Leica Geosystems. Theoretically, the usefulness of staggered arrays depends from spatial resolution, which is defined by the total point spread function of the imaging system and Shannon's sampling theorem. Due to the two shifted sensor lines staggering results in a doubled number of sampling points perpendicular to the flight direction. In order to simultaneously double the sample number in the flight direction, the line readout rate, or integration time, has to produce half a pixel spacing on ground. Staggering in combination with a high-resolution optical system can be used to fulfil the sampling condition, which means that no spectral components above the critical spatial frequency 2/D are present. Theoretically, the resolution is as good as for a non-staggered line with half pixel size D/2, but radiometric dynamics should be twice as high. In practice, the slightly different viewing angle of both lines of a staggered array can result in a deterioration of image quality due to aircraft motion, attitude fluctuations or terrain undulation. Fulfilling the sampling condition further means that no aliasing occurs. This is essential for the image quality in quasi - periodical textured image areas and for photogrammetric sub-pixel accuracy. Furthermore, image restoration methods for enhancing the image quality can be applied more efficiently. The panchromatic resolution of the ADS40 optics is optimised for image collection by a staggered array. This means, it transfers spatial frequencies of twice the Nyquist frequency of its 12k sensors. First experiments, which were carried out some years ago, indicated already a spatial resolution improvement by using image restitution the ADS 40 staggered 12k pairs. The results of the restitution algorithm, which is integrated in the ADS image processing flow, has now been analysed quantitatively. This paper presents the theory of high resolution image restitution from staggered lines and practical results with ADS40 high resolution panchromatic images and high resolution colour images, created by sharpening 12k colour images with high resolution pan-chromatic ones.

1. INTRODUCTION

1.1 High Resolution Digital Cameras

Recent technology developments provide new solutions for high-resolution image acquisition for photogrammetric applications. These cameras are based on large CCD-matrices as well as CCD-line sensors and allow for a large field of view and a high spatial resolution. Single- or multi-line cameras have been designed for spaceborne, airborne and terrestrial scanners to provide high-resolution wide angle or even panoramic imagery. Such cameras allow new approaches of 3D scene visualization and reconstruction as well as new applications in airborne and close range photogrammetry.
In the last few years first commercial available digital mapping cameras like Leica ADS40 (Sandau, 2000), ZI/Imaging DMC (Hinz, 2000) and Vexcel Ultracam (Leberl, 2003) become available.

1.2 CCD-line cameras and staggered CCD-line arrays

Resolution improvement is a scientific topic for imaging since more than 20 years. Sampling and resolution issues can be found e.g. in (Holst, 1998). For staring arrays, the sampling frequency is created by the detector center-to-center spacing. The effective sampling frequency can be increased with microscan or dither technique in one or two directions. To increase the sampling rate, the scene can be mechanically or optically dithered. By these means the image is augmented by an additional set of samples with an offset relative to the initial set by half the width of the detector elements.
With linear scanning systems, the detector output in scan direction can be electronically digitized at any rate. The only limitation results from the sensor sensitivity required to achieve an appropriate signal to noise ratio (SNR). In cross scan direction, the sampling rate for single linear arrays is defined by the detector size. Using an additional array and shifting the detectors, any vertical Nyquist frequency can be created (Holst, 1998). Figure 1 shows this situation for an ideal undisturbed scan using single and a staggered array. For a single linear array the detector size Δ_{pix} is equal to the sampling distance δ_{pix}. The sampling limit or Nyquist frequency is $1/2\delta_{pix}$. In the case of staggered arrays the sampling distance is half of the pixel size and therefore the sampling limit is extend to $1/\delta_{pix}$.

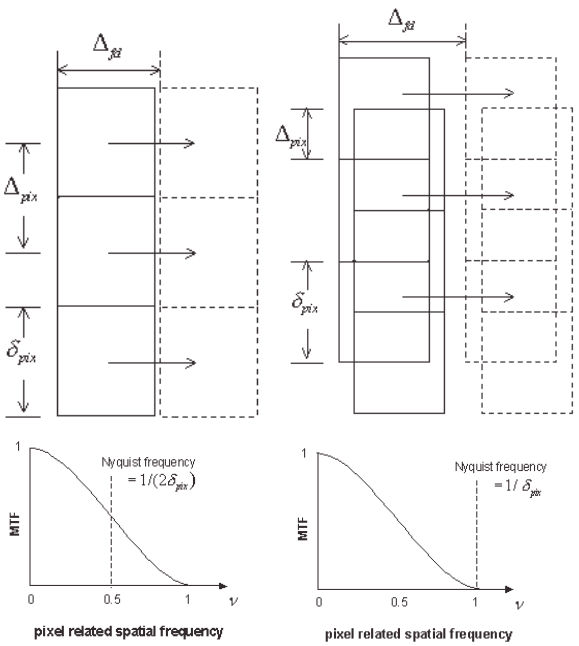

Figure 1. Sampling and Nyquist frequency for linear and staggerd CCD-line

1.3 Restoration

The staggered array approach improves the SNR due to a four times lager pixel size but deteriorates the point spread function. Therefore image restoration is necessary to realize the interior resolution of the images. Digital image restoration is a field of engineering that studies methods used to recover an original scene from degraded observation. The solution is based on estimation theory and the solution of ill-posed inverse problems. Techniques used for image restoration are oriented toward modelling the degradation, usually blur and noise, and applying an inverse procedure to obtain an approximation of the original scene.

1.4 Sampling and Resampling

Line scan data are influenced by flight movement. The result is a variable stochastically disturbed sampling pattern on ground. An additional randomly distributed change of sampling pattern is due to topographic changes. To combine image data of both staggered lines, a resampling and interpolation algorithm is required. Image and sensor quality can be measured by the evaluation of test structures in the image.
The organization of the paper is as follows. We start with an overview about the ADS40 camera, image resolution and improvement techniques and the resolution potential of staggered lines. The third chapter describes the experiment, data evaluation and results.

2. CCD-LINE CAMERAS AND STAGGERED CCD-LINE ARRAYS

2.1 The Camera System ADS40

The ADS40 is based on the tree-line principle. CCD line sensors provide a high ground resolution combined with a large swath width.

The ADS40 has seven parallel sensor lines - three panchromatic lines (forward, nadir, backward), three colour lines (red, green blue) and one near infrared - in the focal plane of a single lens system. The three panchromatic sensor lines produce the forward, nadir and backward views along the strip. This yields the stereo angles shown in table 1. Each panchromatic line consists of two linear arrays, each with 12000 pixels, but staggered by 0.5 pixels as shown in figure 1. The colour lines (red, green, blue), each 12000 pixels long, are optically superimposed by a dichroitic beam splitter. The great advantage of this approach is that the colour image is band registered without significant postprocessing. The near infrared sensor lines are 12000 pixels long and slightly offset from the RGB triplet. The precise position of each pixel is known after the calibration process.
Because of the linear sensor structure, the second dimension of the image is generated by the aircraft movement and is influenced by attitude disturbances. To correct this effect, exact attitude and position measurements are necessary for each image scan line being realised by an Inertial Measurement Unit (IMU) mounted directly to the camera body.
During the flight, imagery, GPS position data, IMU data and other house-keeping data are written to a removable disk pack.
In order to assure the desired high number of detector elements per line, staggered arrays are used. These detectors consist of two single 12k CCD lines positioned with a across-track shift of half a pixel to each other.

Table 1 shows the most important parameters of the camera.

Focal length	62.7 mm
Pixel size	6.5 µm
Panchromatic line	2 x 12.000 pixels
Colour lines	12.000 pixels
Field of View (across track)	64 °
Stereo angles	16°, 26°, 42°
Dynamic range	12 bit
Radiometric resolution	8 bit
Ground sampling distance (3000 m altitude)	16 cm
Swath width (3000 m altitude)	3.75 km
Read out frequency per CCD line	200 – 800 Hz
In flight storage capacity	600 GByte

Table 1. Parameters of the ADS40 camera

2.2 Image Degradation

Images are degraded by both blur and additive noise. The blur can be described in terms of the Point Spread Function (PSF) and is caused e.g. by the atmosphere, motion of the object or the system, defocusing of the optics, finite size of the aperture, the detector and so on. The measured signal in a linear model is the convolution of the object radiance with the system PSF. Additional noise will be superposed by the detector and preamplifier.
The sampled signal values $I'(x_i,y_j)$ ($x_i = i\cdot\Delta$, $y_j = j\cdot\Delta$, i,j = 0, ±1, ±2,.) can be obtained by a convolution of I(x,y) with the geometrical pixel PSF

$$I'(x_i, y_j) = \iint H(x_i - x', y_j - y') \cdot I(x', y')\, dx'\, dy' + \xi(x_i, y_j)$$

H(x,y) is the space invariant point spread function, I(x,y) the scene on detector pixel position $x=i\Delta_1$, $y=j\Delta_2$, and ξ the noise of the imaging system. With abbreviation $f_{i,j}=f(i\Delta_1,j\Delta_2)$ follows

$$I'_{i,j} = \int\int dx'dy'\, H\left(i\Delta_1 - x', j\Delta_2 - y'\right)\cdot I\left(x', y'\right) + \xi_{i,j}$$

The $\xi_{i,j}$ are uncorrelated random numbers with zero expectation value:

$$\left\langle \xi_{i,j} \right\rangle = 0 \quad \left\langle \xi_{i,j}\, \xi_{k,l} \right\rangle = \sigma^2 \cdot \delta_{i,k} \cdot \delta_{j,l}$$

Image restoration means the estimation of the scene brightness $I'(x_i,y_j)$ on the position $x'_i=i\delta_1$, $y'_2 = j\delta_2$ with $\delta_1 \le \Delta_1$, $\delta_2 \le \Delta_2$. For $\delta < \Delta$ we have subpixel accuracy.

To simplify for the integral we use discrete scalar notation. With approximation of the scene with a step function it follows

$$I'_{i,j} = \sum_{k,l} h(i-k, j-l)\cdot I_{k,l} + \xi_{i,j} = \sum_{k,l} h_{k,l}\cdot I_{i-k,j-l} + \xi_{i,j}$$

For pixel resolution ($\mu=\nu=1$) is

$$I'_{i,j} = \sum_{k,l} h_{k,l}\cdot I_{i-k,j-l} + \xi_{i,j}$$

and for the 1D case

$$I'_i = \sum_{k,l} h_k \cdot I_{i-k} + \xi_i$$

It is meaningful to fit most of the PSF with a Gaussian shape function

$$h_{i,j} = c\cdot \exp\left\{ -\frac{(x-x_0)^2}{\sigma_x^2} - \frac{(y-y_0)^2}{\sigma_y^2} \right\}$$

Because of different pixel size for the focal plane arrays, a reference of the PSF to pixel distance is meaningful. Typical values for sigma of the system-PSF are in the range of 0.5 to 1.0 in units of pixel size in the image plane. An approximate determination of the PSF includes optics and the pixel size. An additional part in moving direction must be taken into account. The following calculation is done only in one dimension. The pixel PSF for the most simple case (constant sensitivity, no diffusion effects) is

$$H_{pix}(x) = \begin{cases} \dfrac{1}{\delta} & if \quad -\dfrac{\delta}{2} \le x \le \dfrac{\delta}{2} \\ 0 & elsewhere \end{cases}$$

The optics PSF can be model with a Gaussian shape function with $\sigma \approx \delta/3$. Figure 2 shows the resulting MTF and its components for the ADS40. The motion MTF depends on flight height and should be in the range of half of a pixel.

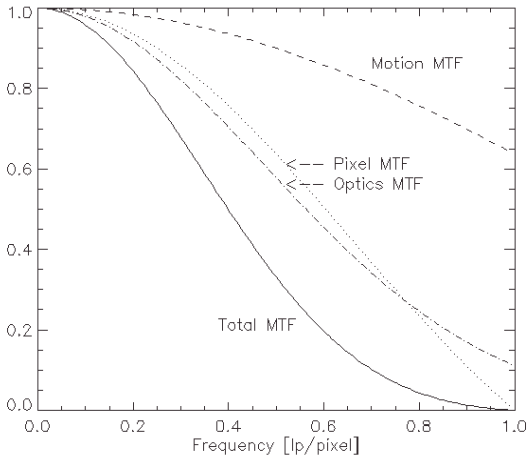

Figure 2. MTF-estimation for ADS40

2.3 Image Restoration

The removal of blur has been investigated with great effort in the past (Andrews and Hunt, 1977; Katsaggelos, 1991). Image restoration is an ill-posed inverse problem. For this reason, a unique solution may not exist, and a small amount of noise can lead to large reconstruction errors. To overcome this difficulty, a priori knowledge on the original scene and PSF as well as noise information on the image forming system are necessary.

Image reconstruction approaches may be distinguished by the derivation criteria, by algorithms working in the object and Fourier space, by local, recursive and global algorithms, by linear and non linear algorithms, and so on. The applied algorithm for blur removal depends on the special application, the prior information and the used criterion for the restoration quality as well as on system PSF and noise. Some examples are: Inverse Filter, Least-Squares Filter, SVD-Based Pseudo-Inverse Filter, Maximum Entropy Pseudo-Inverse Filter, Laplacian-Constrained Least-Squares Filter and Linear Minimum Mean-Square Error Wiener Filter (see Katsaggelos, 1991).

The algorithm to be used here is the linear restoring finite impulse response (FIR) filter, described e.g. in (Reulke, 1995). The FIR or local filter is a fast algorithm to estimate the original grey value from the surrounding image values. Since the algorithm is a local one, local changes of the camera properties (PSF and noise) or the scene statistics may be considered. For filter coefficient determination the least mean square solution (LMS) should be used.

The scene is described as a stationary random process which contains the prior information for stabilization of the reconstruction problem. For the estimation of the scene value at position i,j we use the linear FIR filter approach

$$\hat{I}_{i,j} = \sum_{k,l} a_{k,l}\cdot I'_{i-k,j-l}$$

The unknown coefficients are determined by minimizing the least mean square error

$$\Im(a) = \left\langle \left[\hat{I}_{i,j} - I_{i,j} \right]^2 \right\rangle$$

The derivation to the coefficients leads to a set of linear equations for the optimal filter coefficients a_{kl}. An additional parameter $\varepsilon=\sigma/\kappa$ is essential for stabilizing or regularizing the solution.

2.4 Resolution of staggered CCD-line

To validate the resolution enhancement of staggered arrays theoretical investigations of the ultimate spatial resolution taking into account the total point spread function (PSF) and Shannon's sampling theorem have been carried through. (Jahn, 2000).

Theoretically, the resolution is as good as for a non-staggered line with half pixel size $\Delta/2$ if the pixels of the staggered line array have size $\Delta/2$ too (with pixel distance Δ). The slightly different viewing angle of both lines of a staggered array can lead to deteriorations because of aircraft motion and attitude fluctuations and a non-flat terrain.

The sampling process with respect to a special pixel size shall be described. We are looking for the sampling of the optical signal I(x,y) behind the optics and in front of the focal plane. The sampling is realised by rectangular or square detectors with pixel size $\delta\times\delta$ arranged in a regular line grid with sampling distance Δ. For staggered arrays this distance is given by $\Delta = \delta/2$ (see figure 1).

The signal values $I_{i,j} = I(x_i,y_j)$ ($x_i = i\cdot\Delta$, $y_j = j\cdot\Delta$, i,j = 0, ±1, ±2,.) can be obtained by a convolution of I(x,y) with the geometrical pixel PSF

$$I'\left(x_i, y_j\right) = \int\int H\left(x_i - x', y_j - y'\right)\cdot I\left(x', y'\right) dx'dy'$$

The pixel PSF only in one dimension is

$$H_{pix}(x)=\begin{cases}\frac{1}{\delta} & if \quad -\frac{\delta}{2}\le x\le\frac{\delta}{2}\\ 0 & elsewhere\end{cases}$$

A double point source $\delta(x_0)$, $\delta(x_0+a)$, a is the distance between both point sources, generates an spatially dependent intensity distribution in front of the focal plane $H(x - x_0) + H(x - x_0 - a)$. H(x) is the system PSF without the pixel PSF. The signal in the sampling point $i\cdot\Delta$ is obtained by integrating the optical signal over the pixel area

$$I(i\Delta)=\int_{-\delta/2}^{\delta/2}\left[H(x+i\Delta-x_0)+H(x+i\Delta-x_0-a)\right]dx$$

Assuming a Gaussian-PSF with a "width" (standard deviation) σ, the integration can be performed using Gauß's probability-integral. The result (see Jahn, 2000) is a pixel dependent intensity distribution

$$I(i\Delta)=c\cdot\left\{\Phi\left(i\frac{\Delta}{\sigma}+\frac{\delta}{2\sigma}-\frac{x_0}{\sigma}\right)-\Phi\left(i\frac{\Delta}{\sigma}-\frac{\delta}{2\sigma}-\frac{x_0}{\sigma}\right)+\Phi\left(i\frac{\Delta}{\sigma}+\frac{\delta}{2\sigma}-\frac{x_0+a}{\sigma}\right)-\Phi\left(i\frac{\Delta}{\sigma}-\frac{\delta}{2\sigma}-\frac{x_0+a}{\sigma}\right)\right\}$$

The measured values I(iΔ) depend for a given pixel distance Δ/σ and a pixel size δ/σ (related to the PSF width σ) also on the point position (phase) x_0/σ and on the distance a/σ between the light spots. That means that the accuracy definition or the contrast depends on the displacement of the point source relative to the pixel.

We introduce as a measure for the resolution the a Minimum Resolvable Distance (MRD). In the context of a Rayleigh-criterion based resolution concept, the MRD is the minimum distance of two radiating points to be resolved.

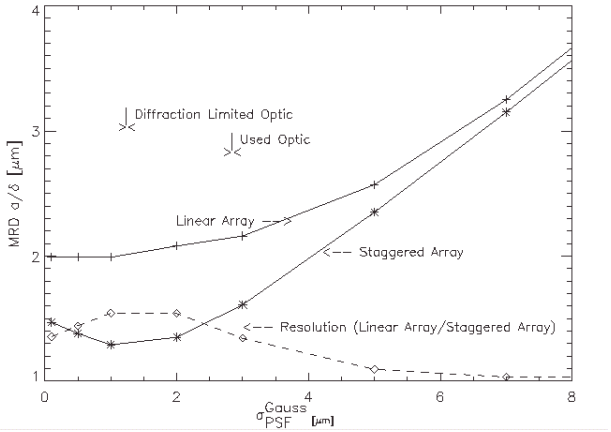

Figure 3. Double point resolution in relation to the optical PSF

Figure 3 shows the resolution in case of double point resolution (distance between the two spots with respect to the pixel size) as a function of the PSF parameter σ (the used optics has a f-number = 4). For the diffraction limited optics the equivalent σ is 1μm (see Jahn, Reulke, 1998) and for the real ADS40 optics we have σ ≈ 2.5μm.

In case of negligible PSF, the limit for the double point accuracy is valid. With increasing PSF-width σ especially for the staggered arrays, the MRD also increases, while the resolution for single arrays keeps constant. We find the minimal MRD for staggered arrays in case of diffraction limited optics. Increasing σ further the MRD becomes worse. Typical values for resolution are in the range of MRD ≈ 3*σ or for the ADS40 camera MRD ≈ 1.5 pixel.

The resolution can be improved by image restoration.

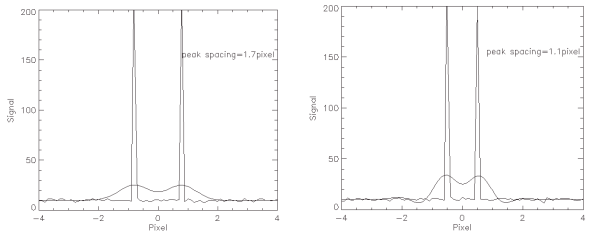

Figure 4. Resolution improvement of restored images

The left image of figure 4 shows an example used for resolution derivation from figure 3. With a σ≅0.5 pixel the minimal resolution in the sense of the Rayleigh criteria is about 1.7 pixel. After applying the restoration algorithm the resolution can be improved by about 30%, which is equivalent to an improvement of the system-PSF.

3. PROCESSING OF THE DATA

The following chapter describes the data reception and processing.

3.1 Processing scheme of ADS40 data

After archiving images, position data and other house-keeping data, the GPS/IMU data is processed with the GPS base station data. This results in position and orientation files which are used to create Level 1 rectified images, which are stereo viewable, ready for processing in many classical remote sensing systems and are used to perform triangulation, compilation, DTM production, etc. Further image analysis products and level 2 rectified greyscale, colour and multispectral orthophotos can also be created.

After the GPS/IMU data has been processed, the position and attitude files and a simplified interior orientation of the camera are used to rectify the images to a ground plane at a user-specified elevation. This allows the correction of the aircraft motion and results in stereo viewable images (Level 1 rectified images). Each rectified image is broken up into large blocks of a user-specified size and can be written in standard formats such as 8-bit TIFF, 16-bit TIFF and tiled TIFF. Furthermore, it is ready for human stereo viewing and point measurement using image matching techniques and other automated processes.

Aerial triangulation is used to combine the short-term accuracy of the IMU with the high global accuracy of GPS. In combination with a minimum number of ground control points, aerial triangulation delivers best fitting results on the ground. The extra information added to the system by tie point measurement leads to very reliable orientation results.

3.2 Data base

For data evaluation we concentrate on a flight over the Rheintal area, which covers a flat region without breaks. This test site is located close to the Leica facilities in Heerbrugg/Switzerland and is typically used for the in-flight calibration of the ADS40 sensor system including camera interior orientation parameters and the spatial relation to GPS/IMU components. The typical calibration flight geometry is similar to the flight pattern of this test, where several crossing strips were collected in different height levels to investigate resolution potential of this data (see figure 5) and to achieve a rigid block geometry for calibration tasks. The

numbers in figure 5 indicate the starting point of each individual flight strip. As it can be seen, the flights are flown in opposite flight directions. Such a flight pattern is necessary to de-correlate different parameters from camera calibration. At the time of writing, detailed data evaluations were available for the two strips 1213 and 1239 in the flight height 1140 m and 950 m only. The terrain height is 450 m. The equivalent ground sampling distance (GSD) for the single CCD-line is 10 cm and 5 cm, respectively.

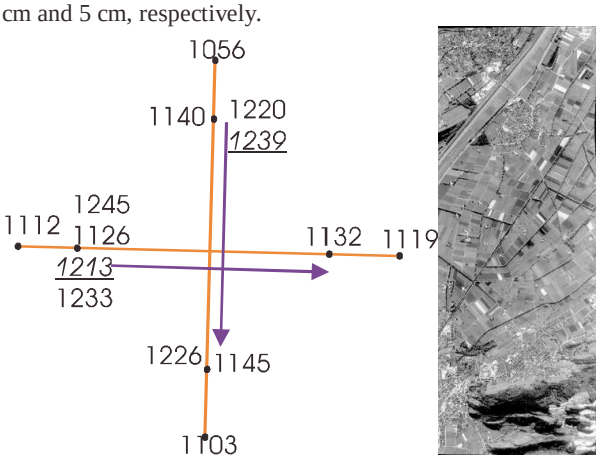

Figure 5. Rheintal calibration block and image example

Image restoration was applied on each original (L0) image of the staggered line. The restoration parameters are derived for this special data set and are σ=0.8 (pixel) for the PSF and ε = 0.07 for the regularization parameter.

3.3 Rectification

For the rectification a horizontal plane located at a mean terrain height is defined (Haala et al, 1998). As indicated in figure 6 below the direct method of image rectification is applied for each of both nadir lines (A and B – line). Each pixel in the image space is projected on the Z–plane using orientation and position of the respective scan line.

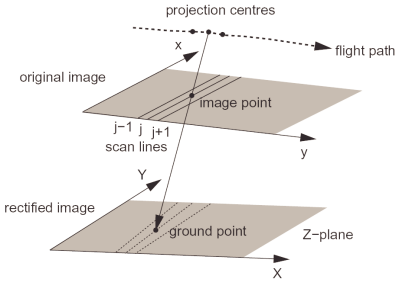

Figure 6. Direct method for image rectification

The resulting ground points are irregularly distributed in this plane and carry the grey value of the corresponding image points.

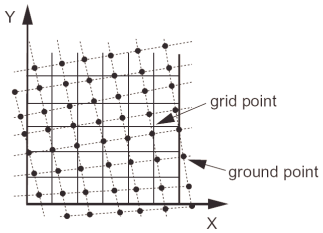

Figure 7. Irregular distribution of image points

For image interpolation the Natural Neighbours approach was selected (Sibson, 1981). For this purpose Natural Neighbours interpolation creates a Delauney triangulation from the irregularly distributed ground points and selects the closest nodes forming a convex hull around each raster point to be interpolated. During interpolation, the grey values of these neighboured points are then weighted according the proportionate areas defined by the resulting Voronoi diagram. This method was selected since Natural Neighbours is accepted as a good general purpose interpolation technique. Investigations on alternative approaches are being performed.

3.4 Sampling pattern calculation

The ideal sampling pattern can be derived from camera and flight conditions. In flight direction it depends from sampling time, flight height and speed. In line direction the sampling depends from pixel distance, camera focal length and flight height. The first data set (1239) has a GSD ???? das stimmt was nicht vermutlich Ergebnisse heute mittag abwarten

Flight track #	Flight height above ground	GSD in CCD-line direction (not staggered / staggered)	GSD in flight direction (not staggered / staggered)
1239	500 m	5cm / 2.5 cm	7 cm / 7 cm
1213	990 m	10 cm / 5 cm	12 cm / 6 cm

Table 2. Relevant parameters for tested data sets

As shown in table 1 the consideration of staggered line results no resolution improvement in flight direction.

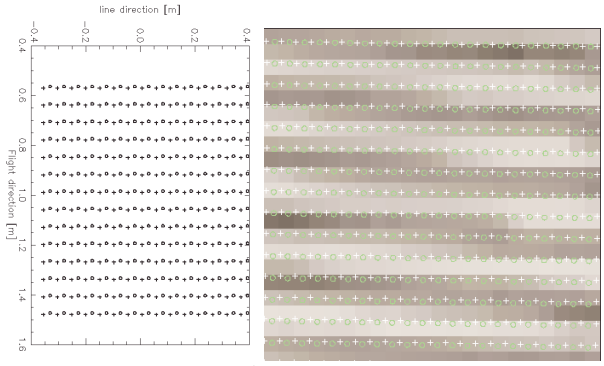

Figure 8. Comparison of calculated and measured sampling pattern for flight track 1239

The interpolation was done on a GSD of 5 cm in flight and line direction. The circle and the cross are related to the A and B nadir line. Figure 8 shows a good agreement of calculated and measured sampling pattern.

3.5 Results

We investigated the resolution of staggered ADS40 images. The original and restored rectified image points are sampled on different geometrical raster. For analysing the resolution and resolution improvement a Siemens star was used.
Figure 9 shows the interpolated resolution pattern before and after image restoration. An improvement of sharpness is visible. Also some artefacts in the bar target are visible, which can be related with under-sampling effects.

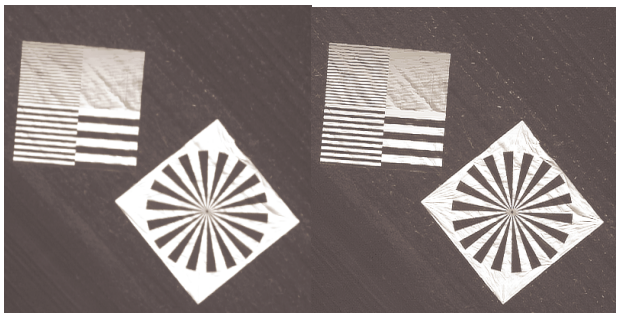

Figure 9. Resolution pattern – bar target and Siemens star. Interpolated (left image) and restored image (right image)

To quantify the resolution and the results of restoration we investigate modulation of different resolution patterns (see figure 10). A convenient approach is the analysis of radial modulation of the Siemens star.

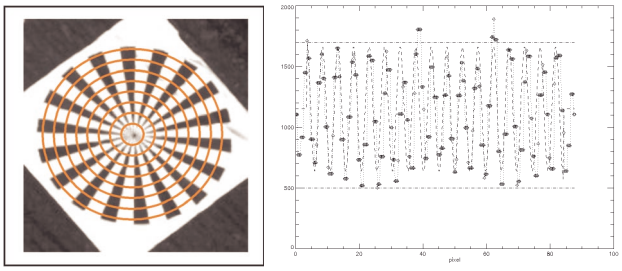

Figure 10. Analysis of modulation from Siemens star (left) with radial modulation analysis for one circle (right)

The diameter of the star in pixel is proportional to circumference of a circle and can be analysed in relation to image pixel. Different diameter realize variable spatial frequencies. The evaluation of the modulation for different radii gives a quantitative prediction for the resolution.

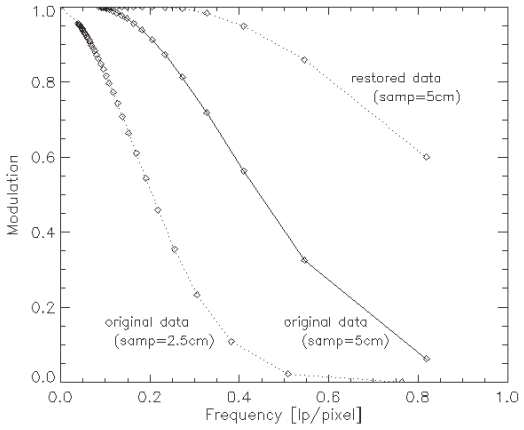

Figure 11. Evaluation of the modulation from Siemens star

In figure 11 the measured data from modulation analysis are shown. The measured data are in a good accordance to a fit on a Gaussian. The original data are sampled on 5 cm and 2.5 cm. The analyses of the Gaussian parameter σ (which is 0.5 pixel for the 5 cm data) shows the expected factor of two between both measures. The influence of restoration before rectification provide an improvement in σ and therefore in resolution, which is also a factor of two. Using resolution definition like in chapter 2.4 the MRD is in the range of 7.5 cm for the original data and better than one pixel for the restored data.

CONCLUSION

The given results from the Rheintal test mission show the large potential of ADS40. The results will be reconfirmed by another test flight, that will be flown in the Vaihingen/Enz test site, maintained from Institute for Photogrammetry (ifp). Besides the verification of resolution potential a second focus is laid on the analysis of the maximum geometric accuracy, which will be evaluated from independent check points in object space. In this context especially the influence of different IMU quality for subsequent data processing is investigated.

ACKNOWLEDGEMENTS

The authors would like to thank Werner Schneider, Susanne Becker and Mathias Schneider for preparation and evaluation of the data.

BILIBOGRAPHY

Andrews, H.C. and Hunt, B.R., 1977. *Digital Image Restoration*", Englewood Cliffs, New Jersey

Haala, N., Stallmann, D., Cramer, M., 1998, Calibration of directly measured position and attitude by aerotriangulation of three-line airborne imagery, in: T. Schenk & A. Habib, eds, *ISPRS Commission III Symposium on Object Recognition and Scene Classification from Multispectral and Multisensor Pixels*, Columbus/Ohio, USA, pp. 23-30.

Hinz, A., 2000. Digital Modular Camera: System Concept and Data Processing Workflow, In: *The International Archives of the Photogrammetry, Remote Sensing and Spatial Information Sciences*, Amsterdam, Vol. XXXIII, Part B2. pp. 164.

Holst, G.C., 1998, *Sampling, Aliasing, and Data Fidelity for Electronic Imaging Systems, Communications, and Data Acquisition*, SPIE-Press

Jahn, H., Reulke,R., 2000, Staggered Line Arrays in Pushbroom Cameras: Theory and Application,International *The International Archives of the Photogrammetry, Remote Sensing and Spatial Information Sciences*, Amsterdam, Vol. XXXIII, Part B1, pp. . 164

Katsaggelos, A.K., 1991. *Digital image restoration*" , - Berlin ; Heidelberg : Springer

Leberl F., 2003, The UltraCam Large Format Aerial Digital Camera System. *Proceedings of the ASPRS Annual Convention*, Anchorage / Alaska, USA, May 5-9 (CD only).

Reulke, R., 1995, Comparison of image reconstruction algorithms, *Remote Sensing and Reconstruction for Three-Dimensional Objects and Scenes*, SPIE 2572-14, p.126

Sandau, R., 2000, Design Principles of the LH Systems ADS40 Airborne Digital Sensor, In: *The International Archives of the Photogrammetry, Remote Sensing and Spatial Information Sciences*, Amsterdam, Vol. XXXIII, Part B2, pp. 552.559.

Sibson, R., 1981, A brief description of natural neighbour interpolation. In V. Barnet, (ed) Interpreting Multivariate Data John Wiley & Sons, pp. 21 - 36